$A_2[MX_4]$ Copper(II) Pyridinium Salts. From Ionic Liquids to Layered Solids to Liquid Crystals

Francesco Neve,*,† Oriano Francescangeli,‡ Alessandra Crispini,† and Jonathan Charmant§

Dipartimento di Chimica, Università della Calabria, I-87030 Arcavacata di Rende (CS), Italy, Dipartimento di Scienze dei Materiali e della Terra, and Istituto Nazionale per la Fisica della Materia, Università di Ancona, Via Brecce Bianche, I-60131 Ancona, Italy, and School of Chemistry, University of Bristol, Bristol BS8 1TS, United Kingdom

Received October 9, 2000. Revised Manuscript Received March 22, 2001

The synthesis and characterization of a novel series of tetrachlorocuprate salts, based on *N*-alkylpyridinium cations ([C*n*−Py]$^+$), are described. The [C*n*−Py]$_2$[$CuCl_4$] salts ($n = 6, 9-18$) were found to be crystalline solids except for the short-chain homologues ($n = 6, 9, 10$), which were obtained as viscous liquids. X-ray powder diffraction measurements showed that in the crystalline state the ionic species give rise to layered structures. An X-ray crystal structure study of [C15−Py]$_2$[$CuCl_4$] also confirmed the lamellar packing and revealed the monolayer type of organization with strong interdigitation and canting of *N*-alkyl chains. Most solid salts ($n \geq 12$) are thermotropic liquid crystals, with hexagonal columnar, cubic, and smectic phases appearing in the order of increasing chain length and/or temperature. This unique phase behavior has been undoubtedly proved by optical, calorimetric, and diffractometric techniques. The details of the structural organization in both the columnar and cubic phases are not entirely defined yet.

Introduction

Amphiphilic organic species such as *n*-alkyl-substituted phosphonate, sulfate, carboxylate, phosphonium, or ammonium ions are widespread molecular components of supramolecular frameworks of varying dimensionality.[1−4] Whereas the most extensive use of such species (especially *n*-alkylammonium ions) is currently directed toward the design of new mesoporous materials,[5−8] a great deal of investigation on these systems is still devoted to the synthesis of layered solids by way of self-assembly,[9] intercalation,[10,11] or exchange reactions.[12] In the layer structure, the organic component basically acts as a modulator of the interlayer distance, thereby affording a modulation of specific properties (e.g., magnetism, conductivity, or superconductivity) as desired.[13,14]

Layered $A_2[MX_4]$ salts, where A is an organoammonium ion (A_2 may also be an organodiammonium ion) and X is a halide, have long been known either for their thermal[15−19] (M = Mn, Fe, Co, Cu, Zn, Cd, Hg) or for their magnetic[20−26] (M = Cr, Mn, Fe, Cu) behavior. More recently, photoluminescence and dielectric properties have been exploited for M = Ge, Sn, Pb, and Eu.[27−39]

* To whom correspondence should be addressed. E-mail: f.neve@unical.it.
† Università della Calabria.
‡ Università di Ancona.
§ University of Bristol.

(1) Clearfield, A. *Prog. Inorg. Chem.* **1998**, *47*, 371.
(2) Thompson, M. E. *Chem. Mater.* **1994**, *6*, 1168.
(3) Kimizuka, N.; Kunitake, T. *Adv. Mater.* **1996**, *8*, 89.
(4) Coombs, N.; Khushalani, D.; Oliver, S.; Ozin, G. A.; Shen, G. C.; Sokolov, I.; Yang, H. *J. Chem. Soc., Dalton Trans.* **1997**, 3941.
(5) Kresge, C. T.; Leonowicz, M. E.; Roth, W. J.; Vartuli, J. C.; Beck, J. S. *Nature* **1992**, *359*, 710.
(6) Huo, Q.; Margolese, D. I.; Ciesla, U.; Feng, P.; Gier, T. E.; Sieger, P.; Leon, R.; Petroff, P. M.; Schuth, F.; Stucky, G. D. *Nature* **1994**, *368*, 317.
(7) Huo, Q.; Margolese, D. I.; Ciesla, U.; Demuth, D. G.; Feng, P.; Gier, T. E.; Sieger, P.; Firouzi, A.; Chmelka, B. F.; Schuth, F.; Stucky, G. D. *Chem. Mater.* **1994**, *6*, 1176.
(8) Barton, T. J.; Bull, L. M.; Klemperer, W. G.; Loy, D. A.; McEnaney, B.; Misono, M.; Monson, P. A.; Pez, G.; Sherer, G. W.; Vartuli, J. C.; Yaghi, O. M. *Chem. Mater.* **1999**, *11*, 2633.
(9) Era, M.; Hattori, T.; Taira, T.; Tsutsui, T. *Chem. Mater.* **1997**, *9*, 8.
(10) Ogawa, M.; Takizawa, Y. *Chem. Mater.* **1999**, *11*, 30.
(11) Choy, J.-H.; Kwon, S.-J.; Hwang, S.-J.; Kim, Y.-I.; Lee, W. *J. Mater. Chem.* **1999**, *9*, 129.
(12) Laget, V.; Hornick, C.; Rabu, P.; Drillon, M. *J. Mater. Chem.* **1999**, *9*, 169.
(13) Laget, V.; Hornick, C.; Rabu, P.; Drillon, M.; Ziessel, R. *Coord. Chem. Rev.* **1998**, *178−180*, 1533.
(14) Ogawa, M.; Kuroda, K. *Chem. Rev.* **1995**, *95*, 399.
(15) Vacatello, M.; Corradini, P. *Gazz. Chim. Ital.* **1973**, *103*, 1027.
(16) Vacatello, M.; Corradini, P. *Gazz. Chim. Ital.* **1974**, *104*, 773.
(17) Landi, E.; Vacatello, M. *Thermochim. Acta* **1975**, *12*, 141.
(18) Landi, E.; Vacatello, M. *Thermochim. Acta* **1975**, *13*, 441.
(19) Kind, R.; Plesko, S.; Arend, H.; Blinc, R.; Zeks, B.; Seliger, J.; Lozar, B.; Slak, J.; Levstik, A.; Filipic, C.; Zagar, V.; Lahajnar, G.; Milia, F.; Chapuis, G. *J. Chem. Phys.* **1979**, *71*, 2118.
(20) Needham, G. F.; Willett, R. D.; Franzen, H. F. *J. Phys. Chem.* **1984**, *88*, 674.
(21) Mostafa, F. M.; Willett, R. D. *Phys. Rev.* **1971**, *B3*, 2213.
(22) De Jongh, L. J.; Miedema, R. *Adv. Phys.* **1974**, *23*, 1.
(23) Phelps, D. W.; Losee, D. B.; Hatfield, W. E.; Hodgson, D. J. *Inorg. Chem.* **1976**, *15*, 3147.
(24) Bellitto, C.; Day, P. *J. Chem. Soc., Dalton Trans.* **1978**, 1207.
(25) Willett, R. D.; Place, H.; Middleton, M. *J. Am. Chem. Soc.* **1988**, *110*, 8639, and references therein.
(26) Zhou, P.; Drumheller, J. E.; Rubenacher, G. V.; Halvorson, K.; Willett, R. D. *J. Appl. Phys.* **1991**, *69*, 5804.
(27) Dolzhenko, Y. I.; Inabe, T.; Maruyama, Y. *Bull. Chem. Soc. Jpn.* **1986**, *59*, 563.
(28) Ishihara, T.; Takahashi, J.; Goto, T. *Solid State Commun.* **1989**, *69*, 933.
(29) Ishihara, T.; Takahashi, J.; Goto, T. *Phys. Rev. B* **1990**, *42*, 11099.
(30) Calabrese, J.; Jones, N. L.; Harlow, R. L.; Herron, Thorn, D. L.; Wang, Y. *J. Am. Chem. Soc.* **1991**, *113*, 2328.

10.1021/cm000804d CCC: $20.00
Published on Web 05/17/2001

Although a few structural studies revealed the presence of isolated $[MX_4]^{2-}$ ions (for M = Cu or Zn),[40−44] most salts have a layered perovskite structure[45] with two-dimensional (2D) inorganic regions interleaved between organic layers.[23,25,27−35,39,46−50] Magnetic coupling, which is mainly intralayer, thus strongly benefits from such a structural motif.[45,51] Moreover, tuning of the degree of corrugation of the inorganic sheets can be achieved through control of the stereochemistry of the organic moieties.[52]

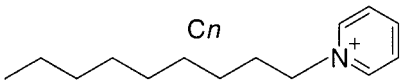

$[Cn\text{-Py}]^+$, $n = 6, 9–18$

Unlike organoammonium salts, $A_2[MX_4]$ salts containing heterocyclic cations substituted with *n*-alkyl chains have attracted much less attention.[11,53−56] Structural evidence is even more sparse,[53,55] thus making any comparison with the organoammonium series far out of reach. We have recently begun to fill the gap by starting a systematic study on $A_2[MX_4]$ salts of *N*-alkylpyridinium cations (designated as $[Cn-Py]^+$) and $[PdX_4]^{2-}$ anions.[55,57] Our aim was to increase the number of structural studies to establish relationships between the physical properties of the salts and their layer packing motifs. The choice of pyridinium cations was dictated by the fact that (i) they can be easily prepared, (ii) their incorporation may trigger liquid crystal behavior when *n*-alkyl tails of appropriate length are chosen,[55,57,58] and (iii) they may lead to technologically important metal-based ionic liquids.[59−61] In addition, although the substituted pyridinium cations do have a weak hydrogen-bonding donor capability,[62] the importance of chlorometalate ions as strong hydrogen-bonding acceptors has been asserted[63] and has found interesting applications.[64−66] This combination calls for an additional factor controlling the final structure beyond those inherent to the different halometalate anions (i.e., the type of metal and its tendency toward a specific coordination geometry).

Here, we present a study on a series of *N*-alkylpyridinium salts of $[CuCl_4]^{2-}$, an ion with potential (more or less distorted) tetrahedral or octahedral coordination when participating in organic−inorganic perovskite-like structures.[45] The study shows, depending on the length of the alkyl chain on the pyridinium cation, the $[Cn-Py]_2[CuCl_4]$ (n = 6, 9−18) salts are room-temperature liquids (n = 6, 9, 10) or layered solids (n = 11−18), respectively. The latter may also behave as thermotropic liquid crystals, whose phase behavior has been extensively investigated. Within the group of liquid crystalline terms (n = 12−18) a remarkable variety of liquid crystal phases was observed. These range from lamellar phases (with the usual smectic A structure) to columnar phases or even to cubic phases. Yet in the present case the conventional correlation between the appearance of a specific mesophase and the increasing number of carbon atoms in the peripheral alkyl chains seems to be overturned.

Experimental Section

Materials. All reactions and manipulations were performed in air with reagent-grade solvents. The pyridinium chlorides [C12−Py][Cl] and [C16−Py][Cl] were purchased as monohydrate salts (Aldrich) and used as received. The pyridinium chlorides, which were not commercially available, were obtained in high yield through a procedure already reported for some of the them[55] and recrystallized from pyridine−diethyl ether. The recrystallized chloride salts usually take up a water molecule as shown by ^{1}H NMR spectroscopy. [C9−Py][Cl] is a yellow-brown jelly, whereas [C6−Py][Cl] is a yellowish oil.

Techniques. Elemental analyses were performed with a Perkin-Elmer 2400 microanalyzer by the Microanalytical Laboratory at the Università della Calabria. Optical observations were carried out with a Zeiss Axioskop polarizing microscope equipped with a Linkam CO-600 heating stage and a temperature control unit. Phase transition temperatures were measured by differential scanning calorimetry (DSC) with a Perkin-Elmer DSC-7 instrument operating at a scanning rate of 5 °C/min. Sample pans were kept in a dry nitrogen atmosphere.

Powder X-ray diffraction (PXRD) measurements at different temperatures were performed with a Bruker AXS General Area Detector Diffraction System (GADDS) with monochromatized Cu Kα radiation. Indexing of the powder patterns was performed using the Cerius^2 program.[67]

(31) Mitzi, D. B.; Feild, C. A.; Harrison, W. T. A.; Guloy, A. M. *Nature* **1994**, *369*, 467.
(32) Mitzi, D. B.; Wang, S.; Feild, C. A.; Chess, C. A.; Guloy, A. M. *Science* **1995**, *267*, 1473.
(33) Mitzi, D. B. *Chem. Mater.* **1996**, *8*, 791.
(34) Mitzi, D. B.; Liang, K. *Chem. Mater.* **1997**, *9*, 2990.
(35) Mitzi, D. B.; Chondroudis, K.; Kagan, C. R. *Inorg. Chem.* **1999**, *38*, 6246.
(36) Chondroudis, K.; Mitzi, D. B. *Chem. Mater.* **1999**, *11*, 3028.
(37) Papavassiliou, G. C.; Koutselas, J. B. *Synth. Met.* **1995**, *71*, 1713.
(38) Papavassiliou, G. C. *Prog. Solid State Chem.* **1997**, *25*, 125.
(39) Mousdis, G. A.; Papavassiliou, G. C.; Raptopoulou, C. P.; Terzis, A. *J. Mater. Chem.* **2000**, *10*, 515.
(40) Ciajolo, M. R.; Corradini, P.; Pavone, V. *Acta Crystallogr.* **1977**, *B33*, 553.
(41) Zuniga, F. J.; Chapuis, G. *Cryst. Struct. Commun.* **1981**, *10*, 533.
(42) Avitabile, G.; Ciajolo, M. R.; Napolitano, R.; Tuzi, A. *Gazz. Chim. Ital.* **1983**, *113*, 475.
(43) Place, H.; Willett, R. D. *Acta Crystallogr.* **1988**, *C44*, 34.
(44) Bond, M. R.; Johnson, T. J.; Willett, R. D. *Can. J. Chem.* **1988**, *66*, 963.
(45) For a recent review on organic−inorganic perovskites, see: Mitzi, D. B. *Prog. Inorg. Chem.* **1999**, *48*, 1.
(46) Guo, N.; Lin, Y.-H.; Xi, S.-Q. *Acta Crystallogr.* **1995**, *C51*, 617.
(47) Steadman, J. P.; Willett, R. D. *Inorg. Chim. Acta* **1970**, *4*, 367.
(48) Peterson, E. R.; Willett, R. D. *J. Chem. Phys.* **1972**, *56*, 1879.
(49) Halvorson, K.; Willett, R. D. *Acta Crystallogr.* **1988**, *C44*, 2071.
(50) Sekine, T.; Okuno, T.; Awaga, K. *Inorg. Chem.* **1998**, *37*, 2129.
(51) Day, P. *J. Chem. Soc., Dalton Trans.* **1997**, 701.
(52) Guan, J.; Tang, Z.; Guloy, A. M. *Chem. Commun.* **1999**, 1833.
(53) Hitchcock, P. B.; Seddon, K. R.; Welton, T. *J. Chem. Soc., Dalton Trans.* **1993**, 2639.
(54) Bowlas, C. J.; Bruce, D. W.; Seddon, K. R. *Chem. Commun.* **1996**, 1625.
(55) Neve, F.; Crispini, A., Armentano, S.; Francescangeli, O. *Chem. Mater.* **1998**, *10*, 1904.
(56) Choy, J.-H.; Kwon, S.-J.; Park, G.-S. *Science* **1998**, *280*, 1589.
(57) Neve, F.; Crispini, A.; Francescangeli, O. *Inorg. Chem.* **2000**, *39*, 1187.
(58) Bowlas, C. J.; Bruce, D. W.; Seddon, K. R. *Chem. Commun.* **1996**, 1625.
(59) Chauvin, Y.; Olivier-Bourbigou, H. *CHEMTECH* **1995**, *25* (9), 26.
(60) Freemantle, M. *Chem. Eng. News* **1998**, *76* (13), 32.
(61) Carmichael, H. *Chem. Br.* **2000**, *36* (1), 36.
(62) Aakeröy, C. B.; Seddon, K. R. *Chem. Soc. Rev.* **1993**, 397.
(63) Aullón, G.; Bellamy, D.; Brammer, L.; Bruton, E. A.; Orpen, A. G. *Chem. Commun.* **1998**, 653.
(64) Barbour, L. J.; MacGillivray, L. R.; Atwood, J. L. *Supramol. Chem.* **1996**, *7*, 167.
(65) Lewis, G. R.; Orpen, A. G. *Chem. Commun.* **1998**, 1873.
(66) Gillon, A. L.; Orpen, A. G.; Starbuck, J.; Wang, X.-M.; Rodríguez-Martín, Y.; Ruiz-Pérez, C. *Chem. Commun.* **1999**, 2287.
(67) *CERIUS^2 3.0 Molecular Simulations Program*; Molecular Simulations Inc.: San Diego, CA, 1997.

Synthesis of the Tetrachlorocuprates [C*n*−Py]$_2$[CuCl$_4$] (*n* = 6, 9−10). An orange solution of $CuCl_2 \cdot 2H_2O$ (0.086 g, 0.5 mmol) and the appropriate *N*-alkyl pyridinium chloride (1.0 mmol) in acetonitrile (6 mL) was heated under reflux for 30 min. Evaporation of the solvent (either under reduced pressure or in air) then afforded a viscous orange-brown liquid, which had no tendency to crystallize at room temperature.

Synthesis of the Tetrachlorocuprates [C*n*−Py]$_2$[CuCl$_4$] (*n* = 11−18). The complete series of solid salts [C*n*−Py]$_2$[CuCl$_4$] (*n* = 11−18) has been obtained in a similar way to that followed for the lower homologues. Solid $CuCl_2 \cdot 2H_2O$ (0.1 g, 0.59 mmol) was added to a colorless solution of the appropriate *N*-alkyl pyridinium chloride (1.18 mmol) in acetonitrile (10 mL). Heating the resulting yellow solution to reflux for 30 min led to a darkening of the color. Golden yellow needles or plates formed either by cooling the orange-brown solution to room temperature (higher *n* values) or freezing it down to −18 °C (lower *n* values). Yields were usually very high, as was the purity of the products. Yields are listed along with the corresponding analytical data for all the salts (*n* = 11−18).

n = 11. Yield, 91%. Anal. Calcd for $C_{32}H_{56}Cl_4CuN_2$: C, 57.01; H, 8.37; N, 4.16. Found: C, 56.60; H, 8.31; N, 3.96.

n = 12. Yield, 63%. Anal. Calcd for $C_{34}H_{60}Cl_4CuN_2$: C, 58.19; H, 8.62; N, 3.99. Found: C, 57.82; H, 8.48; N, 4.03.

n = 13. Yield, 86%. Anal. Calcd for $C_{36}H_{64}Cl_4CuN_2$: C, 59.21; H, 8.83; N, 3.84. Found: C, 58.82; H, 8.78; N, 4.02.

n = 14. Yield, 85%. Anal. Calcd for $C_{38}H_{68}Cl_4CuN_2$: C, 60.68; H, 9.04; N, 3.69. Found: C, 59.92; H, 8.73; N, 4.12.

n = 15. Yield, 95%. Anal. Calcd for $C_{40}H_{72}Cl_4CuN_2$: C, 61.09; H, 9.23; N, 3.56. Found: C, 60.71; H, 9.11; N, 4.05.

n = 16. Yield, 84%. Anal. Calcd for $C_{42}H_{76}Cl_4CuN_2$: C, 61.94; H, 9.40; N, 3.43. Found: C, 61.24; H, 9.50; N, 3.82.

n = 17. Yield, 98%. Anal. Calcd for $C_{44}H_{80}Cl_4CuN_2$: C, 62.73; H, 9.57; N, 3.33. Found: C, 62.29; H, 9.68; N, 3.35.

n = 18. Yield, 91%. Anal. Calcd for $C_{46}H_{84}Cl_4CuN_2$: C, 63.47; H, 9.72; N, 3.22. Found: C, 62.99; H, 9.64; N, 3.13.

Crystal Structure Determination of [C15−Py]$_2$[CuCl$_4$]. Yellow needles of [C15−Py]$_2$[CuCl$_4$] with relatively poor crystal habit crystallized at room temperature by slow evaporation from an acetonitrile solution. Different conditions of crystallization gave no better results. Data collections at different temperatures were carried out on a Siemens *R*3*m*/*v* diffractometer using graphite-monochromated Mo Kα (λ = 0.71073 Å) radiation (at room temperature) and a Bruker SMART diffractometer (λ = 0. 71073 Å) equipped with a CCD area detector (at 173 K). Several attempts to obtain both a unique crystal class and set of cell parameters carried out on different specimens were unsuccessful. From the room-temperature (293 K) collections, depending on the reflection sets used to index the pattern and the algorithm used for the indexing, two unit cells were obtained: a triclinic [*a* = 7.243(2) Å, *b* = 16.015(5) Å, *c* = 20.654(8) Å, α = 101.18(3)°, β = 91.86(3)°, γ = 89.99(3)°, and *V* = 2349(1) Å^3] and a monoclinic *C*, [*a* = 40.13(1) Å, *b* = 7.955(2) Å, *c* = 7.231(3) Å, β = 91.72(3)°, and *V* = 2308(1) Å^3]. From the low-temperature (173 K) collection, the unit cell obtained was monoclinic *P* with parameters of *a* = 7.284(2) Å, *b* = 16.032(5) Å, *c* = 19.029(9) Å, β = 92.38(6)°, and *V* = 2220(2) Å^3. Because the results are all consistent with twinning, several reflection data sets were used for the formulation of the crystal structure of this species. The details of the best partial structure solutions and refinements, obtained in both the monoclinic *C*2 (room temperature) and *P*2$_1$/*m* (173 K) space groups, are reported in Table 1. Full crystallographic details are available as Supporting Information. The structure solutions and full-matrix least-squares refinements based on F^2 were perfomed with the XS and XL routines in the SHELXTL-NT program package.

Room-Temperature Determination. Copper, chlorine, nitrogen, and the pyridinium carbon atoms were refined anisotropically. Hydrogen atoms were included as idealized atoms riding on the respective carbon atoms with C−H bond lengths appropriate to the carbon atom hybridization. One of the chlorine atoms of $[CuCl_4]^{2-}$ lies at a site of C_2 symmetry, leading to an occupancy of 50.15% for the copper and the other chlorine atoms. The severe disorder on the anion appears clearly from the bond lengths and angles, which reveal a strong deviation from those of a regular tetrahedral molecule.

Low-Temperature Determination. All non-hydrogen atoms were refined anisotropically. Copper and two chlorine atoms lie on a mirror plane. In this structure solution the disorder affects the aliphatic chain of the cation. Apart from the α-carbon, every C atom of the chain is disordered over two sites. Only hydrogen atoms of the pyridinium aromatic ring were included in the final refinement as idealized atoms.

Table 1. Crystallographic Data[a] for [C15−Py]$_2$[CuCl$_4$]

formula	$C_{20}H_{36}Cl_2Cu_{0.5}N$	
fw	393.2	
T (K)	293(2)	173(2)
crystal size	0.08 × 0.4 × 0.35	0.3 × 0.2 × 0.1
crystal system	monoclinic	monoclinic
space group	*C*2	*P*2$_1$/*m*
a (Å)	40.131(8)	7.284(2)
b (Å)	7.955(2)	16.032(5)
c (Å)	7.231(1)	19.029(9)
α (deg)	90.00	90.00
β (deg)	91.71(3)	92.38(6)
γ (deg)	90.00	90.00
V (Å^3)	2308(1)	2220(1)
Z	4	4
ρ_{calcd} (g cm^{-3})	1.132	1.176
λ(Mo Kα) (Å)	0.71073	0.71073
μ (mm^{-1})	0.731	0.760
θ range (deg)	2.0−24.1	1.7−27.5
data collected	2144 [*R*(int) = 0.026]	22646 [*R*(int) = 0.162]
observed data	1969	5276
no. of refined params	157	334
$R^{b,c}$ indices [$I > 2\sigma(I)$]	R_1 = 0.0797 wR_2 = 0.2465	R_1 = 0.0832 wR_2 = 0.2052
R (all data)	R_1 = 0.1277 wR_2 = 0.2803	R_1 = 0.1637 wR_2 = 0.2422
GOF on F^2	0.941	1.032

[a] From data collections at different temperatures. [b] $R_1 = \Sigma||F_o| - |F_c||/\Sigma|F_o|$. [c] $wR_2 = \{\Sigma[w(F_o^2 - F_c^2)^2]/\Sigma[w(F_o^2)^2]\}^{1/2}$.

Results and Discussion

Synthesis. Copper(II) chloride readily reacts with *N*-alkyl pyridinium chlorides [C*n*−Py][Cl] (molar ratio 1:2) in acetonitrile, affording the yellow or orange-brown salts [C*n*−Py]$_2$[CuCl$_4$] (*n* = 6, 9−18), which are soluble in polar solvents such as acetone or acetonitrile. Although the very same salts can be obtained warming the solid reagents in the reaction flask, to prevent the incorporation of cocrystallized water molecules into the products (both the metal halide and the organic salts are hydrated) and to favor the crystallization process, it is preferable to carry out the reaction in refluxing acetonitrile. All the higher homologues (*n* ≥ 11) crystallize out of the reaction mixture and are obtained as air-stable golden yellow needles or plates. Slow diffusion of diethyl ether through acetone solutions of the lower homologues (*n* ≤ 10) cooled at approximately −20 °C leads to the formation of thin yellow needles. However, if the temperature is raised to room temperature, the solid redissolves and no crystallization occurs upon either solvent evaporation, standing for a long period of time, or both. In fact, the [C*n*−Py]$_2$[CuCl$_4$] salts are room-temperature liquids for *n* ≤ 10 (neat samples have appreciable mobility for temperatures as low as 10−15 °C). They are indeed very viscous orange-brown liquids with viscosity decreasing with *n*. No attempts were made to measure the liquid range of the room-temperature liquids because the appropriate apparatus for

Table 2. Phase Behavior of [C*n*−Py]$_2$[CuCl$_4$] (*n* = 6, 9−18)[a]

n	phase transition	*T*	Δ*H*
6	liquid		
9	liquid		
10	liquid		
11	K−I	48.8	21.2
12	K−Col	54.0	29.3
	Col−I	75.8	0.5
13	K−Col	65.6	60.1
	Col−I	90.3	0.7
14	K−K′	51.7	8.9
	K′−Col	68.5 (68.4)[b]	34.3 (45.6)[b]
	Col−I	95.4 (95.0)[b]	0.8 (0.6)[b]
15	K−Cub	77.1	89.3
	Cub−SmA	104.6	0.7
	SmA−I	143.5	0.3
16	K−K′	66.5	15.2
	K′−SmA	78.9 (77.2)[b]	51.7 (47.1)[b]
	SmA−I	180(dec)	
17	K−SmA	85.5	89.5
	SmA−I	211(dec)	
18	K−K′	74.2	37.7
	K′−SmA	83.8 (81.4)[b]	41.4 (45.5)[b]
	SmA−I	209(dec)	

[a] The transition temperatures (°C) and enthalpies (kJ mol^{-1}) were taken from the first DSC heating run unless otherwise specified (scan rate 5 °C min^{-1}). K, K′, crystalline phases; Col, columnar phase; Cub, cubic phase; Sm, smectic phase; I, isotropic phase. [b] Data in parentheses are from the second DSC heating run.

thermogravimetric analysis and subambient calorimetry were not available in our laboratories.

All the members of the [C*n*−Py]$_2$[CuCl$_4$] series (*n* = 6, 9−18) immediately dissolve in water, affording pale blue solutions containing both the hydrated copper(II) and pyridinium cations, thus ruling out any possible use of the salts in water.

Thermotropic Behavior. The phase behavior of the series [C*n*−Py]$_2$[CuCl$_4$] (*n* = 11−18) (i.e., the crystalline members of the whole series) was investigated by polarizing optical microscopy, differential scanning calorimetry (DSC), and X-ray diffraction on powder samples (PXRD). Phase transition temperatures along with the corresponding enthalpy values are summarized in Table 2. A phase diagram is also reported in Figure 1.

All the eight crystalline members of the series exhibited thermotropic polymorphism, except the lowest term (*n* = 11). [C11−Py]$_2$[CuCl$_4$] melted into an isotropic liquid below 50 °C, and no mesophase was observed upon either heating or cooling. For *n* > 11 all the terms showed at least two different phases and, as a general trend, it can be observed that the clearing temperatures steadily increase with increasing length of the alkyl chain with one exception (Figure 2), the term with an octadecyl tail (*n* = 18) whose clearing (actually decomposition) temperature is lower than that for *n* = 17. The variation of the melting temperature with increasing chain length is much less pronounced and it follows an odd−even alternating trend (i.e., the increase is larger from an even to an odd number of C atoms than vice versa).

Going into more detail, the group of mesomorphic copper(II) salts can be divided into three different subsets with regard to their mesogenic behavior. The first subset contains the terms with *n* = 12−14 and represents species that melt into an enantiotropic viscous mesophase whose optical texture appeared as

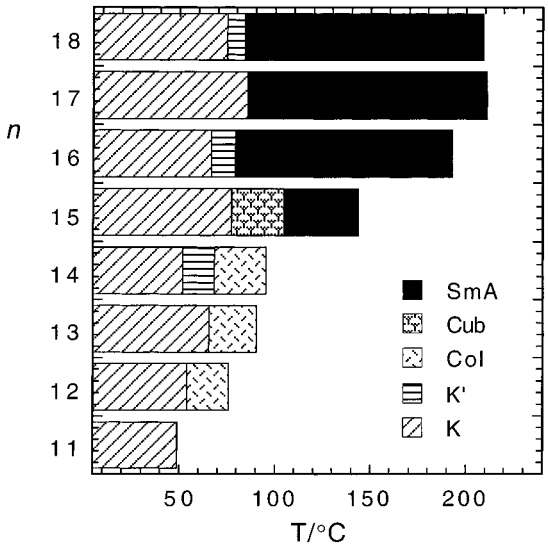

Figure 1. Phase diagram for the series [C*n*−Py]$_2$[CuCl$_4$] (*n* = 11−18).

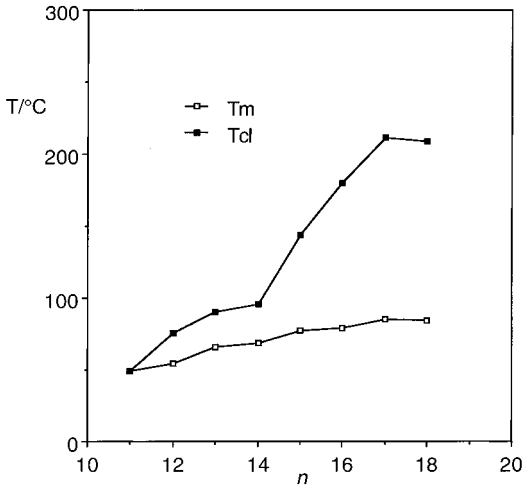

Figure 2. Comparison of the melting transition temperature (T_m) and isotropization temperature (T_{cl}) vs the number of carbon atoms (*n*) in the aliphatic chain of [C*n*−Py]$_2$[CuCl$_4$] (*n* = 11−18).

well-developed fan-shaped focal conics, best seen upon cooling from the isotropic liquid (Figure 3). In one case (*n* = 14), the DSC first heating cycle revealed also a second crystalline phase which was not seen in the second heating cycle.

The salt [C15−Py]$_2$[CuCl$_4$] has unique behavior, showing the phase sequence crystal−cubic−smectic−isotropic liquid. The presence of the cubic phase was preliminarily based on optical microscopic observations. Upon heating, a pristine sample of [C15−Py]$_2$[CuCl$_4$] melted into a very viscous, optically isotropic phase, which upon further heating was replaced by a much less viscous mesophase. The latter appeared under crossed polarizers as birefringent oily streaks interspersed with large pseudo-isotropic areas, a feature characteristic of smectic A phases for the related palladium(II) species.[55,57] Upon cooling from the isotropic liquid, transient spherulitic domains appeared, which were followed by a focal conic texture of uniform distribution. Upon

(68) Demus, D.; Richter, L. *Textures of Liquid Crystals*; Verlag Chemie: Weinheim, 1978.

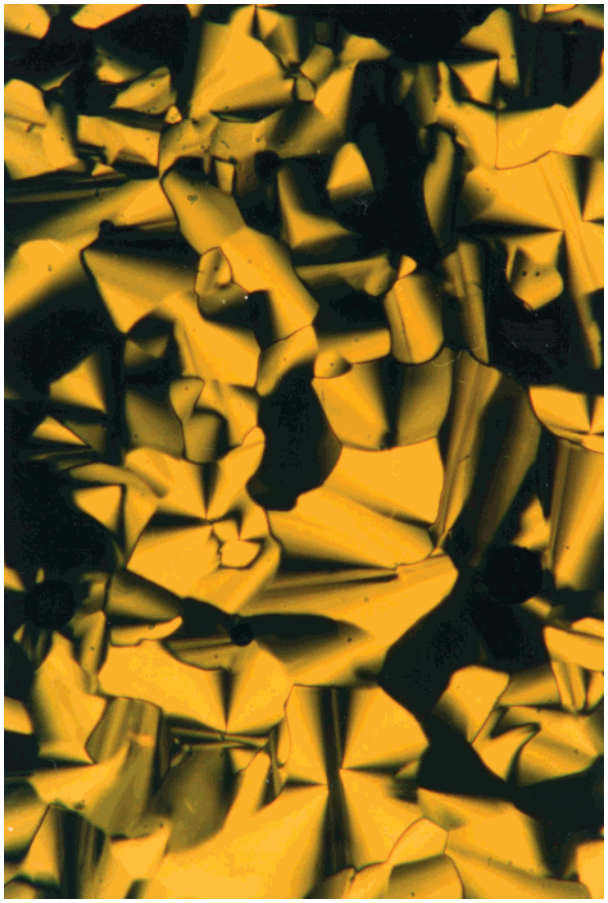

Figure 3. Optical texture observed for $[C12-Py]_2[CuCl_4]$ through crossed polarizers upon cooling from the isotropic liquid to 71 °C.

further slow cooling, growing isotropic areas with a distinctive shape[68] started to form. In particular, the presence of straight edges and the absence of grain boundaries were noted (Figure 4). Eventually, the crystalline phase began to develop before the entire field of view became completely dark. These observations could be fully reproduced for several thermal cycles. It is also useful to note the very small enthalpy value for the cubic-SmA transition (0.7 kJ mol^{-1}), as compared to that for the crystal-cubic one (89.3 kJ mol^{-1}), and the large hysteresis (about 20 °C) with which the nucleation of both the cubic phase and the crystalline phase takes place upon cooling from the smectic phase.

The phase diagrams of the last subset of copper salts (n = 16−18) are characterized by the presence of a single mesophase, which spans a rather wide temperature range (ΔT = 100−130 °C). Optical observations pointed toward a lamellar smectic A phase, which always appeared as oily streaks or small focal conics floating in a homeotropic fluid field. Interestingly, the interference colors of the oily streaks rapidly changed with temperature. As observed by DSC, the subsequent transition to the isotropic liquid was accompanied by extensive decomposition for all three salts. By contrast, samples prepared for optical observation (i.e., confined between a slide and a coverslip) always exhibited a greater stability, with decomposition observed only after more than one thermal cycle and at higher temperatures. As for n = 14, a second crystalline phase was detected by DSC above room temperature in the first heating cycle of the salts with n = 16 and 18.

Figure 4. Micrographs showing the SmA−Cub phase transition for $[C15-Py]_2[CuCl_4]$ as seen through crossed polarizers upon cooling from the smectic phase. From top to bottom: (top) nucleaction of the cubic phase at 82 °C; (following plates) continued transition.

Structural Characterization. (1) Characterization of Crystalline Solids. The structural organization of the crystalline state was studied by PXRD. The powder X-ray diffraction patterns displayed a few reflections at low angles and several reflections in the wide-angle region, as expected for three-dimensional ordered solids. All the patterns were of sufficient quality to give accurate results in the indexing process, but for n = 18. Indexing of the experimental data always converged in the triclinic crystal system, and the corresponding calculated lattice parameters are reported in Table 3. The crystalline solid has a room-temperature

Table 3. Calculated Lattice Parameters and Experimental Lamellar Spacings (d) for the Crystal Phases of $[Cn-Py]_2[CuCl_4]$ (n = 11−18)

no. of C atoms (n)	a (Å)	b (Å)	c (Å)	α (deg)	β (deg)	γ (deg)	d_{calc} (Å)	d_{obs} (Å)
11	7.56(2)	8.11(2)	16.25(8)	89.9(2)	83.3(2)	78.0(2)	16.17	16.18
12	8.33(3)	9.28(1)	17.18(3)	88.7(2)	77.8(1)	86.9(2)	16.79	16.79
13	7.57(2)	10.95(2)	18.29(3)	91.5(1)	93.3(1)	106.3(1)	18.25	18.38
14	8.33(1)[a]	9.45(1)[a]	19.43(1)[a]	90.6(1)[a]	100.0(1)[a]	102.0(1)[a]	19.11[a]	19.15[a]
	8.47(1)[b]	10.98(3)[b]	19.18(4)[b]	95.6(2)[b]	101.4(3)[b]	94.2(1)[b]	18.67[b]	18.69[b]
15	7.12(2)	8.21(4)	20.64(9)	99.1(8)	92.4(6)	90.8(3)	20.31	20.12
16	8.64(6)[a]	9.72(3)[a]	23.32(9)[a]	100.7(3)[a]	97.1(2)[a]	93.4(1)[a]	22.70[a]	22.72[a]
	8.37(4)[c]	10.94(6)[c]	20.73(8)[c]	102.5(3)[c]	96.4(3)[c]	92.5(2)[c]	20.26[c]	20.38[c]
17	7.65(2)	9.45(4)	21.54(1)	78.0(4)	80.4(2)	73.8(2)	20. 95	21.04
18[d]								24.40

[a] From data collected at 20 °C. [b] From data collected at 65 °C. [c] From data collected at 70 °C. [d] Poor quality data.

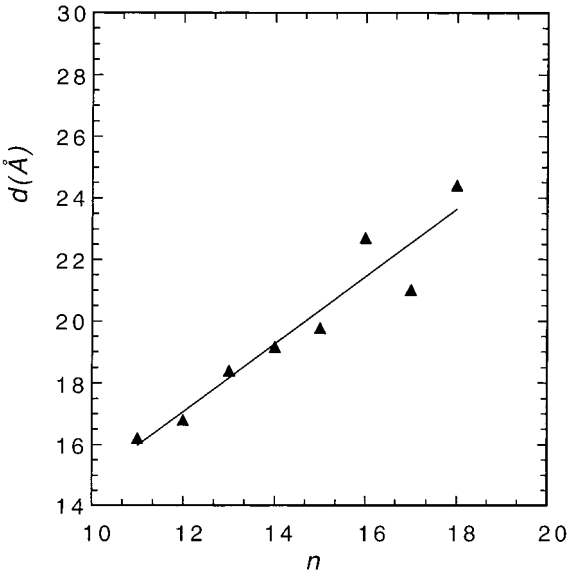

Figure 5. Lamellar periods of the room-temperature crystal phase of $[Cn-Py]_2[CuCl_4]$ (n = 11−18) as a function of the number of carbon atoms in the alkyl chains.

lamellar organization, with observed (and calculated) d-spacings following an almost monotonic trend up to n = 15 (Figure 5). For the higher homologues, the trend becomes different and a tendency toward alternation seems to be established. PXRD experiments also confirmed the lamellar nature of the second crystal phase (K′) revealed by DSC above room temperature for n = 14 and 16 in the first heating run. In the two cases the structural reorganization is not dramatic, although it seems to go along different pathways for the two salts (Table 3).

To assess the importance of the interplay of the different intermolecular interactions (Coulomb attraction and repulsion, hydrogen bonding, van der Waals contacts, hydrophobic interactions) at work in this type of solid, we also attempted to grow single crystals of the copper(II) salts. Only $[C15-Py]_2[CuCl_4]$ gave crystals that apparently were suitable for X-ray analysis, confirming that crystal growth is not an easy task when it comes to the crystallization of salts containing long hydrocarbon side chains in one or both of their ionic components. While experimental evidence of twinning of the crystals makes the analysis of somewhat limited value, nevertheless the discussion will refer to the overall molecular organization and crystal packing, two primary aspects that are of importance for this work and that are not affected to a great extent by low-quality data. The crystal structure of $[C15-Py]_2[CuCl_4]$ consists of discrete cations and anions that are arranged in a lamellar fashion with alternation of hydrophobic and hydrophilic regions along one direction (Figure 6). The cations exhibit alkyl chains with straight, all-transoid conformation. Tilting of the alkyl chains relative to the layer normal results in a layer thickness of 20.06 Å. The disordered $[CuCl_4]^{2-}$ anions are likely involved in several C−H···Cl−M contacts[63,69] with neighboring cations, although their occurrence cannot be asserted with certainty.

Indirect evidence of the absence in these layered solids of two-dimensional infinite layers of interconnected $[CuCl_4]^{2-}$ anions—as observed for perovskite-like structures[45]—came from magnetic measurements. As an example, the temperature dependence of the magnetic susceptibility for $[C15-Py]_2[CuCl_4]$ was measured between 2 and 170 K. The data are consistent with a Curie−Weiss approximation (the corresponding parameters are C = 0.43, θ = −0.25 K, and the average g = 2.14), indicating that the individual anions are magnetically independent over the entire temperature range. In fact, a deviation from Curie−Weiss behavior is observed at very low temperatures (see Supporting Information), which cannot be related to the presence of antiferromagnetic interactions.

Structural Characterization. (2) Characterization of Liquid Crystalline Phases. The structure of the thermotropic liquid crystalline phases was investigated by X-ray diffraction on unaligned powder samples. Upon melting, lower homologues (n = 12−14) showed a similar pattern: that is, a sharp Bragg peak at low angles accompanied by a diffuse reflection in the wide-angle region (Figure 7). The latter (which affords a spacing of 4.6 Å) corresponds to the usual correlation among liquidlike hydrocarbon chains. Further weak reflections in the low−mid-angle region were also revealed, which together with the sharp high-intensity peak, correspond to reciprocal spacings from a two-dimensional hexagonal lattice. Up to five reflections were observed (see n = 12), corresponding to (100), (110), (200), (210), and (300) reflections. The calculated lattice parameters a are reported in Table 4. A second broad reflection can also be seen in the PXRD patterns, which affords a spacing of approximately 7.6 Å in all three cases. This diffuse reflection may represent the stacking period of the cores along the column axis of a columnar hexagonal phase with disordered character. The rather unusual value (if compared to the stacking

(69) Aakeröy, C. B.; Evans, T. A.; Seddon, K. R.; Pálinkó, I. *New. J. Chem.* **1998**, 145.

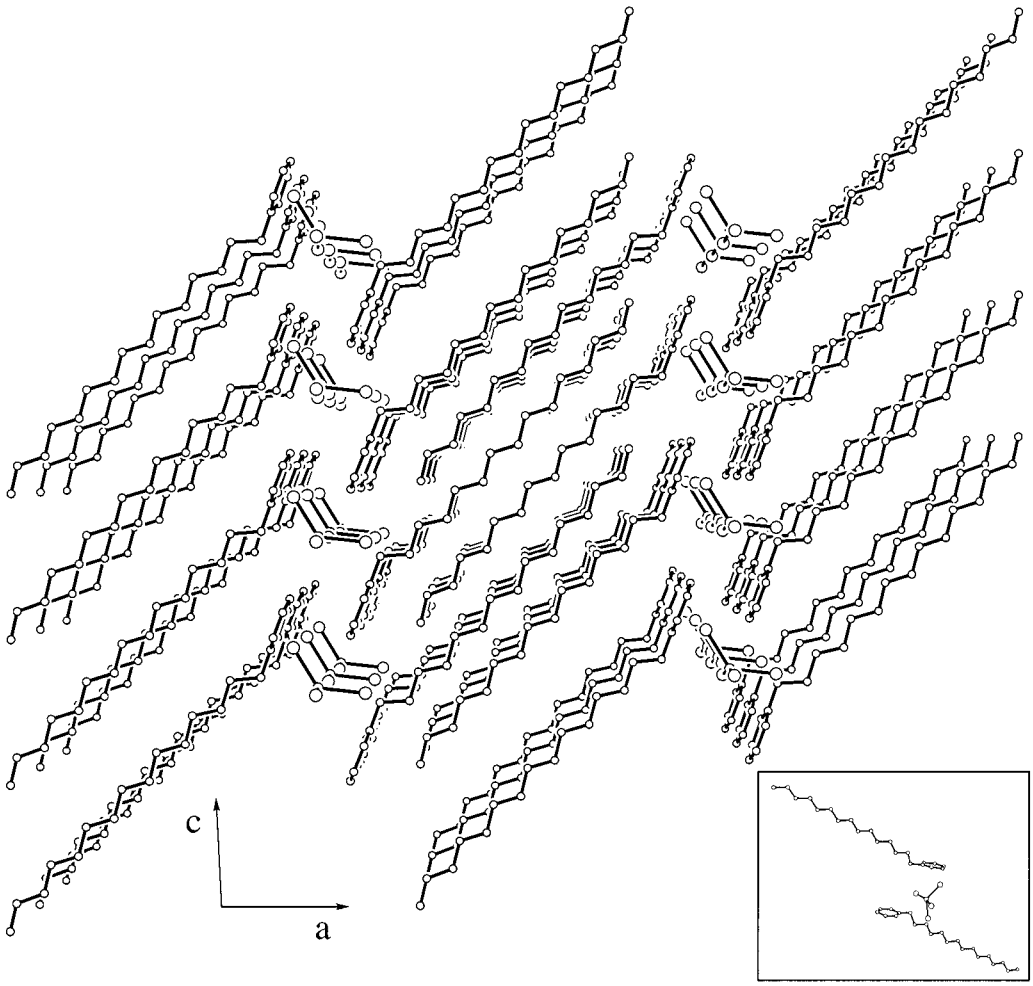

Figure 6. Crystal packing of $[C15-Py]_2[CuCl_4]$ viewed down the *b* axis (monoclinic solution from the room-temperature data collection). The inset contains a view of the asymmetric unit of the same salt.

period for common discotics) may be related to the ionic nature of the molecular constituents as previously observed for ionic thermotropic species.[70]The assignment of the above mesophase as a columnar one seems to be in good agreement with the observation of a common optical texture in the form of well-defined focal conics (see previous section) typical of columnar phases.

The X-ray pattern of the viscous, optically isotropic phase of $[C15-Py]_2[CuCl_4]$ was obtained upon heating the sample above 77 °C and it was identified as that of a primitive cubic phase. Besides a shallow broad feature in the high-angle region, which corresponds to the correlation between liquidlike alkyl chains, the pattern contains up to eight reflections at the relative positions $\sqrt{2}$, $\sqrt{3}$, $\sqrt{4}$, $\sqrt{5}$, $\sqrt{6}$, $\sqrt{8}$, $\sqrt{16}$, and $\sqrt{22}$ (Figure 8, trace B). These reflections can be indexed as the (110), (111), (200), (210), (211), (220), (400), and (332) reflections of cubic symmetry. Because of the intrinsic limitations related to the experimental method and apparatus, it was not possible to assign the pattern to any of the several different noncentered cubic space groups that are compatible with the set of reflections observed. The calculated cubic lattice parameter is 79.6 Å, a value somewhat similar to that obtained for the thermotropic *Ia*3*d* body-centered cubic phase of some alkali metal dihexadecyl phosphates[71] and alkoxystilbazole complexes of silver(I).[70,72] A more detailed structural study is however needed to clarify the exact symmetry of the observed cubic phase. Upon further heating, the cubic phase of $[C15-Py]_2[CuCl_4]$ gives way to a smectic phase with a layer spacing of 30.4 Å (at 115 °C). No further reflections were observed besides a diffuse feature at a wide angle (Figure 8, trace C), which testifies to the disordered character of the phase and the liquidlike conformation of the alkyl chains. In accordance with the observed layer thickness and the optical textures, we assigned the latter phase to a partially bilayer SmA_d type.[73]

Beside the crystalline phases, higher homologues ($n = 16-18$) also exhibit high-temperature XRD patterns consistent with a smectic layering, wherein the layer thickness smoothly follows the corresponding variation of the alkyl side-chain length. On the basis of the diffraction patterns, the structure of the liquid-crystal-

(70) Donnio, B.; Heinrich, B.; Gulik-Krzywicki, T.; Delacroix, H.; Guillon, D.; Bruce, D. W. *Chem. Mater.* **1997**, *9*, 2951.

(71) Tsiourvas, D.; Kardassi, D.; Paleos, C. M.; Gehant, S.; Skoulios, A. *Liq. Cryst.* **1997**, *23*, 269.

(72) Bruce, D. W.; Donnio, B.; Hudson, S. A.; Levelut, A.-M.; Megtert, S.; Petermann, D.; Veber, M. *J. Phys. II (France)* **1995**, *5*, 289.

(73) Seddon, J. M.. In *Handbook of Liquid Crystals*; Demus, D., Goodby, J., Gray, G. W., Spiess, H.-W., Vill, V., Eds.; Wiley-VCH: Weinheim, 1998; Vol. 1, p 635.

(74) Neve, F.; Ghedini, M.; Levelut, A.-M.; Francescangeli, O. *Chem. Mater.* **1994**, *6*, 70.

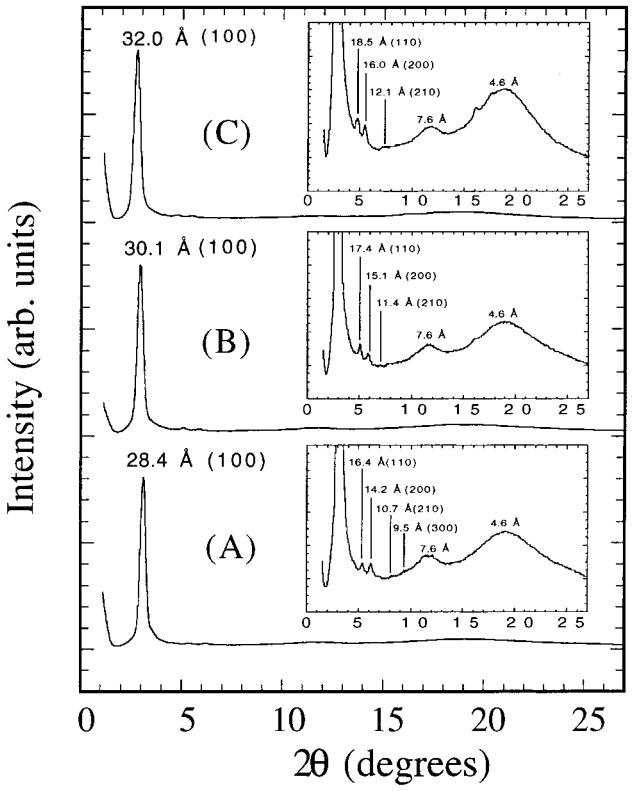

Figure 7. PXRD patterns of [Cn−Py]$_2$[CuCl$_4$] (n = 12−14) in the hexagonal columnar phase, with intensity magnification shown in the insets. (A) n =12, T = 61 °C; (B) n = 13, T = 75 °C; (C) n = 14, T = 75 °C.

Table 4. XRD Data for the Hexagonal Phase of [Cn−Py]$_2$[CuCl$_4$] (n = 12−14)

n	lattice constant (Å)	spacing obs (calcd) (Å)	hkl
12	32.77	28.38	100
		16.40 (16.39)	110
		14.20 (14.19)	200
		10.70 (10.73)	210
		9.50 (9.46)	300
13	34.79	30.13	100
		17.40 (17.40)	110
		15.06 (15.07)	200
		11.40 (11.39)	210
14	36.89	31.95	100
		18.49 (18.45)	110
		16.05 (15.98)	200
		11.86 (12.08)	210

line phase for n = 16−18 is also thought to be of smectic A_d type, a conclusion compatible with the apparent length values for the pyridinium cations (Table 5). Generally, the layer thickness within the SmA_d phases decreases with increasing temperature, a trend already observed for smectic A assemblies of ionic mesogens.[74,75]

In summary, we have seen that the copper(II) salts [Cn−Py]$_2$[CuCl$_4$] (n = 6, 9−18) tend to self-organize in the solid state as layered assemblies provided the hydrocarbon tail of the cations reaches a threshold value ($n \geq 11$). The frustrated crystallization of the terms with intermediate chain length (n = 6, 9, 10) must then be related to a deficient hydrophobic effect, as already noted for 1-alkyl-3-methylimidazolium salts.[76] Upon

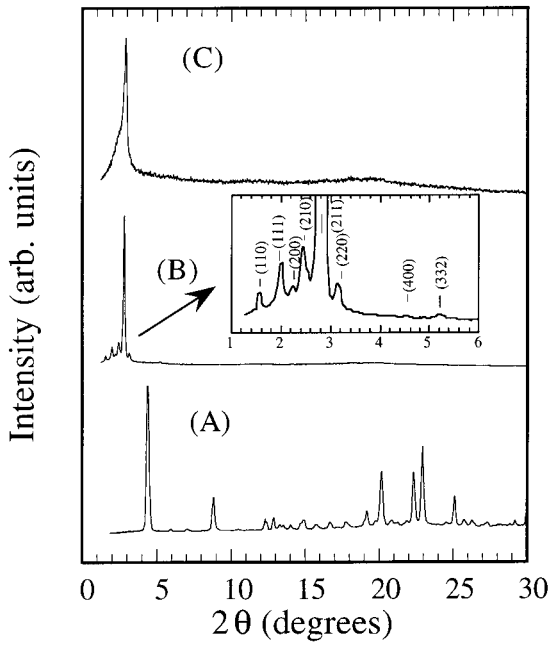

Figure 8. PXRD patterns of [C15−Py]$_2$[CuCl$_4$] recorded at 25 °C (A), 100 °C (B), and 115 °C (C). In (B), the inset represents a magnification of small-angle reflections with the corresponding Miller indices.

Table 5. Spacings (d) for [Cn−Py]$_2$[CuCl$_4$] (n = 12−18) in the Liquid Crystalline Phases as Determined by X-ray Diffraction[a]

	d[b] (Å)			
n	columnar phase	cubic phase	smectic phase	L[c] (Å)
12	28.4 (61)			19.0
13	30.1 (75)			20.3
14	32.0 (75)			21.6
15		56.2[d] (100)	30.4 (115)	22.8
16			33.1 (85)	24.1
17			34.6 (90)	25.3
18			37.1 (90)	26.6

[a] d is either the lamellar period in the smectic phase, the intercolumnar distance in the hexagonal phase, or the spacing corresponding to the 110 reflection in the cubic phase. [b] Temperature (°C) of XRD data collection in parentheses. [c] L is the apparent length of the [Cn−Py]$^+$ pyridinium cations with alkyl chains in the most extended transoid conformation. [d] Cubic cell a parameter = 79.6 Å.

melting, most solid salts ($n \geq 12$) display thermotropic liquid crystalline behavior. In general, they exhibit a single mesophase that can either be lamellar (SmA) or columnar, with the latter prevailing for shorter alkyl chains (Figure 9). This observation seems to be at odds with the common behavior of thermotropic species. First, columnar packing is peculiar to multichain mesogenic molecules or ions, although a discoidal shape is not a prerequisite. For low molecular weight species, and apart from discotics, columnar ordering in the mesophase may also be achieved through pairing of complementary-shaped moieties or clustering of a few mesogenic entities followed by piling of the individual "clusters" into columns (as in phasmids and polycatenar mesogens[77]). Still, the presence of several chains in each single unit is necessary. An additional way leading to columnar ordering occurs for some anhydrous am-

(75) Abdallah, D. J.; Robertson, A.; Hsu, H.-F.; Weiss, R. G. *J. Am. Chem. Soc.* **2000**, *122*, 3053.
(76) Holbrey, J. D.; Seddon, K. R. *J. Chem. Soc., Dalton Trans.* **1999**, 2133.
(77) Malthête, J.; Nguyen, H.-T.; Destrade, C. *Liq. Cryst.* **1993**, *13*, 171.

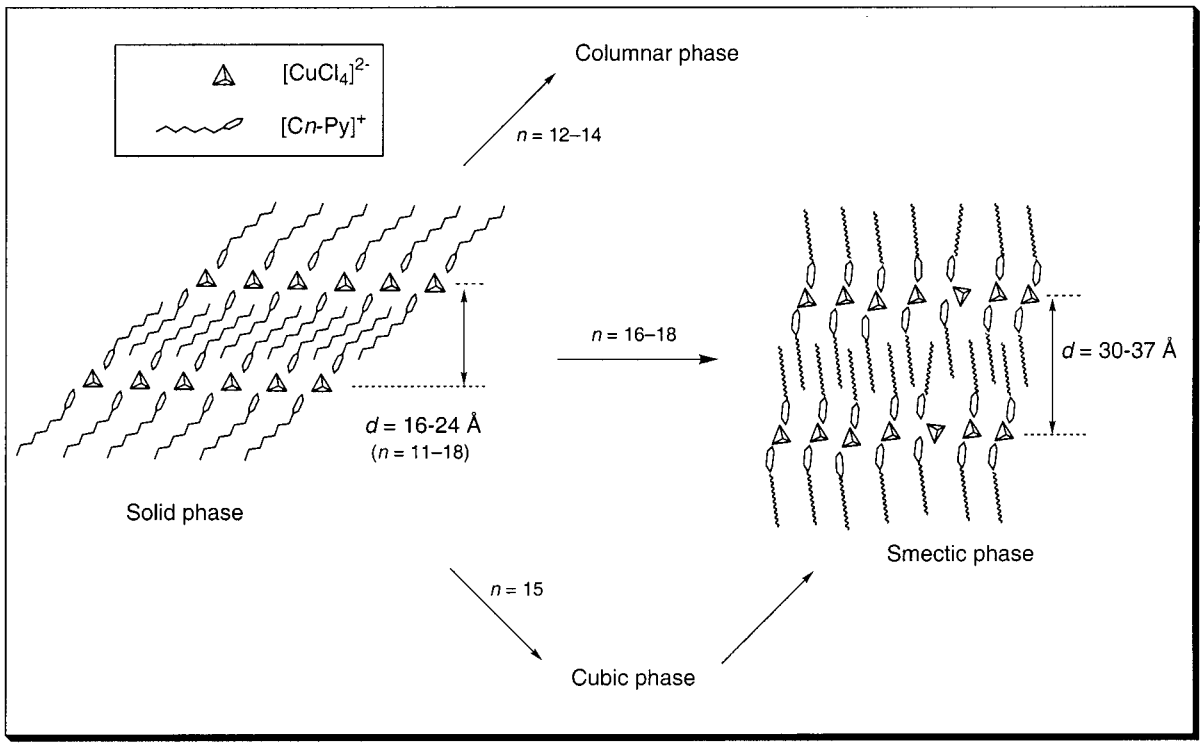

Figure 9. Schematic illustration of thermotropic polymorphism for $[Cn-Py]_2[CuCl_4]$ ($n = 11-18$). The arrows mean increasing temperature, while d represents the layer spacing.

phiphilic systems. Soaps of group 2 metals[78] and primary silver(I)[79] or copper(I)[80] thiolates reportedly form a thermotropic micellar phase with hexagonal columnar simmetry.[81]Thermotropic columnar phases of single-tail amphiphiles are in fact very rare,[82] and few (or none) conclusions could be safely drawn here on how the mesogenic units self-assemble into a rigid (or semirigid) core and how the cores are related along the column axis. While the micellar structural model might fit the experimental data well, we are not aware of the driving force behind it.

The second reason for contrast with the accepted picture of thermotropic liquid crystals is represented by the observed mismatch between side-chain length and supramolecular organization in the mesophase, which apparently subverts the usual molecular structure/surface curvature relationship. The appearance of a given columnar phase in a homologous series is usually associated with longer alkyl chains, with smectic phases (if any) appearing as the chain length decreases. Here, whereas the lamellar structure is the preferred one in the solid state irrespective of the alkyl chain length, in the melt the smectic state is stabilized only by increasing chain length (or with increasing temperature). The mutual organization of anions and cations in the mesophase (other than the smectic one) is likely to be very different from that of the solid. It reverts to the more conventional lamellar ordering for $n \geq 15$ when segregation of the aliphatic parts prevails over other noncovalent interactions.

Finally, a singular point in the polymorphism of $[Cn-Py]_2[CuCl_4]$ salts is represented by the term with $n = 15$. This is the only member of the series displaying two different liquid crystal phases in its phase diagram, one of which is an isotropic cubic phase. Compared to the other homologues, this mesogen presents a more "normal" phase sequence,[83] as upon heating the cubic phase is followed by a smectic A phase.

Conclusions

In this paper we have shown that the series of *N*-alkylpyridinium copper(II) salts reported displays a rather rich polymorphism that, regardless of the unusual features, bring back to mind the even richer polymorphism of alkoxystilbazole complexes of various silver(I) salts studied in depth by Bruce and co-workers.[84] It is interesting to note that both ours and silver(I) systems are ionic, even though the silver species were found to be only formally ionic. Although elusive and somewhat undefined, the role of ionic interactions in promoting a rich mesomorphism should not be underestimated, as has already been pointed out by other authors.[72,85] It is also important to recall that the ability

(78) Spegt, P.; Skoulios, A. *Acta Crystallogr.* **1966**, *21*, 892.
(79) Baena, M. J.; Espinet, P.; Lequerica, M. C.; Levelut, A.-M. *J. Am. Chem. Soc.* **1992**, *114*, 4182.
(80) Espinet, P.; Lequerica, M. C.; Martin-Alvarez, J. M. *Chem. Eur. J.* **1999**, *5*, 1982.
(81) The micellar phase is the thermotropic counterpart of the reversed hexagonal (H_2) lyotropic phase. See, Tiddy, G. J. T. *Phys. Rep.* **1980**, *57*, 1.
(82) Blunk, D.; Praefcke, K.; Vill, V. In *Handbook of Liquid Crystals*; Demus, D., Goodby, J., Gray, G. W., Spiess, H.-W., Vill, V., Eds.; Wiley-VCH: Weinheim, 1998; Vol. 3, p 305.
(83) Diele, S.; Göring, P. In *Handbook of Liquid Crystals*; Demus, D., Goodby, J., Gray, G. W., Spiess, H.-W., Vill, V., Eds.; Wiley-VCH: Weinheim, 1998; Vol. 2B, p 887.
(84) For an early example, see: Bruce, D. W.; Dunmur, D. A.; Hudson, S. A.; Lalinde, E.; Maitlis, P. M.; McDonald, M. P.; Orr, R.; Styring, P.; Cherodian, A. S.; Richardson, R. M.; Feijoo, J. L.; Ungar, G. *Mol. Cryst. Liq. Cryst.* **1991**, *206*, 79. See also refs 70 and 72 for more recent work that specifically addresses cubic phases.
(85) Donnio, B.; Rowe, K. E.; Roll, C. P.; Bruce, D. W. *Mol. Cryst. Liq. Cryst.* **1999**, *332*, 2893.
(86) Neve, F.; Crispini, A.; Francescangeli, O. unpublished results.

of *N*-alkylpyridinium cations to promote extensive H-bonding in the hydrophilic region of the lamellar structure of tetrahalometalates[55,57] may give another clue into the interpretation of the thermal behavior of the salts. Once again, however, the latter observations do not conform well to the observed mesomorphism of *N*-alkylpyridinium salts of different tetrachlorometalate ions (M = Co(II),[54] Ni(II),[54] Pd(II),[55] Zn(II),[86] Cd(II)[86]), which have similar structural characteristics but give rise only to lamellar mesomorphism. The different behavior is certainly related to the nature of the complex metal anion, which in a very subtle way may stabilize (or not) different liquid crystal phases. Exhaustive answers on this point await further investigations.

Acknowledgment. Financial support from the Italian Ministero dell'Università e della Ricerca Scientifica e Tecnologica (MURST) and Consiglio Nazionale delle Ricerche (CNR) is gratefully acknowledged. The authors wish to thank Dr. A. Caneschi (Università di Firenze, Italy) for the magnetic measurements. Thanks are also expressed to F. Cofone (Università della Calabria) for technical assistance.

Supporting Information Available: Two sets of tables of crystal data, structure solution and refinement, atomic coordinates, bond lengths and angles, and anisotropic thermal parameters for $[C15-Py]_2[CuCl_4]$; a perspective view of the asymmetric unit of $[C15-Py]_2[CuCl_4]$ (Figure S1), a view of the crystal structure of $[C15-Py]_2[CuCl_4]$ showing the (C−)H···Cl contacts (Figure S2), and a plot showing the temperature dependence of the magnetic susceptibility for $[C15-Py]_2[CuCl_4]$ (Figure S3) (PDF). An X-ray crystallographic file (CIF). This material is available free of charge via the Internet at http://pubs.acs.org.

CM000804D